

## Synthesis and Anticorrosion Properties of Poly(2,3-dimethylaniline) Doped with Phosphoric Acid

Li Ma, Chao-Qun Huang, Meng-Yu Gan

College of Chemistry and Chemistry Engineering, Chongqing University, Chongqing City 400030, China

Correspondence to: L. Ma (E-mail: mlsys607@126.com)

**ABSTRACT:** Poly(2,3-dimethylaniline) (P(2,3-DMA)) was synthesized chemically by using phosphoric acid ( $H_3PO_4$ ) as protonic acid. The optimum ratio for  $n(H_3PO_4)/n(2,3-DMA)/n(APS)$  was 2.5/1/2, and the optimum temperature was 30°C. The spectra of ultraviolet-visible and infrared demonstrate that the structure of P(2,3-DMA) was similar with polyaniline (PANI) except for the 2,3-ortho-substitute methyl. The result of X-ray diffraction and solubility analysis indicate that owing to the 2,3-ortho-substitute benzene ring, the P(2,3-DMA) has poorly partial crystallinity and better solubility. In addition, the anticorrosion property of P(2,3-DMA) was better than PANI. © 2012 Wiley Periodicals, Inc. *J. Appl. Polym. Sci.* 000: 000–000, 2012

**KEYWORDS:** phosphoric acid; poly(2,3-dimethylaniline); anticorrosion property

Received 26 January 2012; accepted 29 April 2012; published online

DOI: 10.1002/app.37977

### INTRODUCTION

Polyaniline (PANI) has been extensively considered as one of the best useful organic conducting materials because of its good environmental stability, high conducting and optical properties, and protective properties against corrosion.<sup>1–3</sup> However, owing to the stiffness of its backbone, the PANI is difficult to be processed through a traditional method because it is both unstable at melt-processing temperatures and insoluble in most organic solvents except for *N*-methylpyrrolidone (NMP), greatly limiting its further wide practical application.

So, several modifying ways have been developed to improve its solubility. Among them, alkyl, alkoxy, and amino ring-substituted<sup>4–7</sup> and *N*-substituted<sup>8,9</sup> PANIs have caught great interest because of their much better solubility in many common solvents and, therefore, relatively good processibility.

It has been reported that PANI and its derivatives can be used as protective coatings against corrosion, pH sensors, alcohol vapor sensors, and so on.<sup>10–12</sup> 2,3-dimethylaniline is one kind of the derivatives of aniline, has been extensively used as the intermediate of medicine and pesticides. The synthesis of poly(2,3-dimethylaniline) (P(2,3-DMA)) doped with phosphoric acid ( $H_3PO_4$ ) is reported for the first time in this study.

The working electrode was the carbon paper loaded P(2,3-DMA) to analyze the electrochemical properties in this study. The carbon paper was used in the polymerization for two

reasons: (1) to monitor the polymerization reaction at real time, and (2) there already patent and papers confirmed the feasibility of this method.<sup>13</sup>

In this study, the P(2,3-DMA) was synthesized by chemical polymerization using  $H_3PO_4$  as protonic acid media. The effects of the mole ratio of  $H_3PO_4$  to 2,3-dimethylaniline and oxidant (ammonium persulfate, APS) on the electrochemical properties (cyclic voltammogram, Tafel) of P(2,3-DMA) were discussed using the carbon paper loaded P(2,3-DMA) as working electrode, and the yield of P(2,3-DMA) was also investigated. The molecular structure of P(2,3-DMA) was characterized by Fourier transform infrared (FTIR) and ultraviolet-visible (UV-vis) spectroscopies, and X-ray diffraction (XRD) technique. The anticorrosion properties of P(2,3-DMA) was studied by Tafel technique.

### EXPERIMENTAL

#### Preparation of the P(2,3-DMA) and the Working Electrode

$H_3PO_4$ , APS, and all solvents are analytical reagent grades. The P(2,3-DMA) was prepared by chemical polymerization in the presence of  $H_3PO_4$  as doped acid. The polymerization of P(2,3-DMA) is described as follows: 50 mL distilled water containing a calculated amount of  $H_3PO_4$ , 2 mL 2,3-DMA was slowly added into the aqueous solution, and then several pieces of carbon papers (2 cm length and 0.3 cm width) were put into the mixed solution with stirring for 10 min. After that, a precooled solution of APS in 25 mL distilled water was added into the

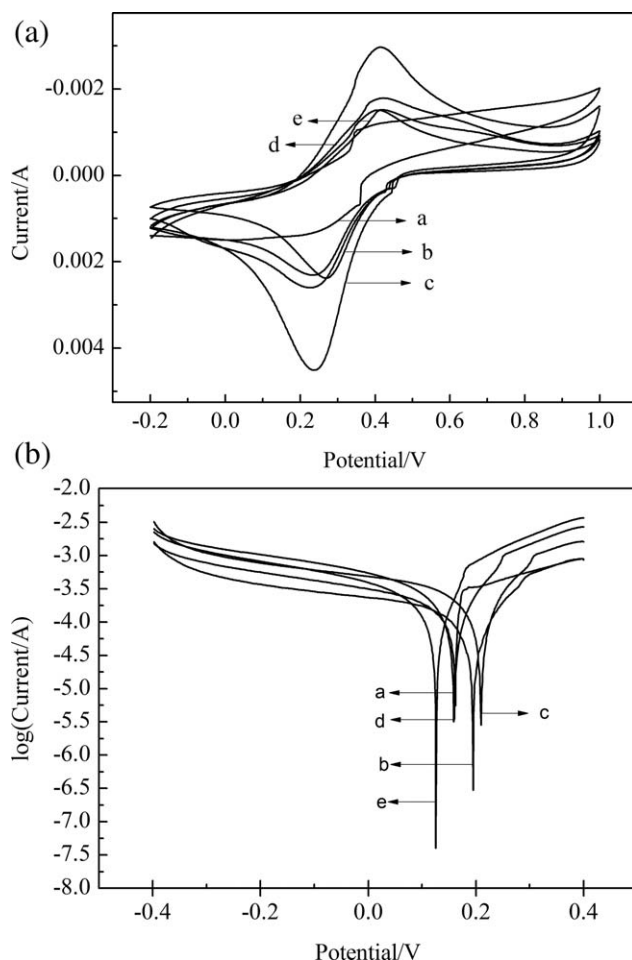


**Figure 1.** CV curves and Tafel polarization curves of P(2,3-DMA) at different mole ratio of  $\text{H}_3\text{PO}_4$  to 2,3-DMA;  $n(\text{H}_3\text{PO}_4)/n(2,3\text{-DMA})$ : a: 1.5 : 1; b: 2 : 1; c: 2.5 : 1; d: 3 : 1; e: 3.5 : 1.

prepared solution under a constant stirring by dropwise. During the progress of polymerization reaction, the color of solution was changing from saffron yellow to purple, and to purple black at last. The reactant solution was magneto-stirred for 9 h until the reaction was completed.

The above obtained solution was filtrated and washed with distilled water until the filtrate was colorless, then dried and obtained the P(2,3-DMA) powder. The carbon papers loaded P(2,3-DMA) were taken out as working electrode for subsequent use.

#### Preparation of the PANI and the Working Electrode

The PANI was synthesized according to the previously described method.<sup>14</sup> At room temperature, a solution containing 2.83 mL  $\text{H}_3\text{PO}_4$  and 2.28 mL aniline was prepared by dissolving in 100 mL 1.0M HCl accompanying with a constant agitation  $\sim 10$  min, and then, several pieces of carbon papers were put into the mixed emulsion with stirring for 10 min. A precooled solution of APS (4.56 g) in 30 mL distilled water was added into the prepared solution under a constant stirring for half an hour by dropwise. The reaction solution was magneto-stirred for 10 h until the reaction was completed.

The above obtained solution was filtrated, and then, the loaded PANI carbon papers were taken out as the working electrode for subsequent use. The PANI powder was obtained after the solution was filtrated, washed, and dried.

#### Characterization

The electrochemical studies were performed with CHI660 electrochemical analyzer under computer control. Electrochemical property tests were performed in a single compartment three-electrode cell with the carbon papers loaded the P(2,3-DMA) or PANI as working electrode, platinum foil as counter electrode, and saturated calomel electrode as reference electrode. Cyclic voltammetry measurement was examined by sweeping the potential from  $-0.2$  to  $1.0$  V at a scan rate of  $20 \text{ mVs}^{-1}$ . Tafel polarization measurement was performed by sweeping the potential between  $-0.40$  and  $0.40$  V at a scan rate of  $10 \text{ mVs}^{-1}$  by potentiodynamic technique.

The P(2,3-DMA) and PANI structure were determined using Shimadzu UV-2.21 PC spectrophotometer in wavelength range between 200 and 900 nm and Nicolet FTIR Model 550II spectrometer with KBr pellets. Wide angle XRD patterns were recorded for the powder polymers with a Shimadzu 6000 X-ray diffractometer in angle range between  $0^\circ$  and  $40^\circ$ . The solubility of P(2,3-DMA) and PANI were qualitatively evaluated using the following method: 0.3 g of fine polymer powders were added into the solvent of 10 mL in a small glass container and ultrasonic oscillation for 10 min at room temperature. Then, the solutions were filtrating and washing with distilled water until the filtrates are colorless, then dried, and obtain the solubility.

## RESULTS AND DISCUSSION

### Synthesis of the P(2,3-DMA)

**Effect of  $\text{H}_3\text{PO}_4$  Concentration.** The effect of the  $\text{H}_3\text{PO}_4$  on the electrochemical property and polymerization yield was studied by varying the mole ratio of  $n(\text{H}_3\text{PO}_4)/n(2,3\text{-DMA})$  from 1.5/1 to 3.5/1 (Figures 1 and 2).

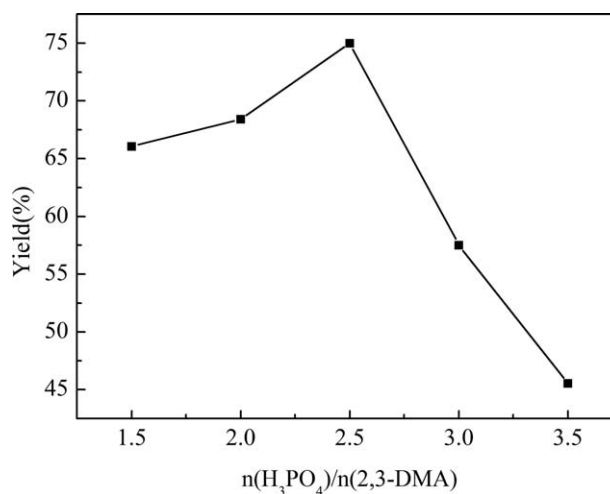


**Figure 2.** The relation between the yield of P(2,3-DMA) and the mole ratio of  $\text{H}_3\text{PO}_4$  to 2,3-DMA;  $n(\text{H}_3\text{PO}_4)/n(2,3\text{-DMA})$ : a: 1.5 : 1; b: 2 : 1; c: 2.5 : 1; d: 3 : 1; e: 3.5 : 1.

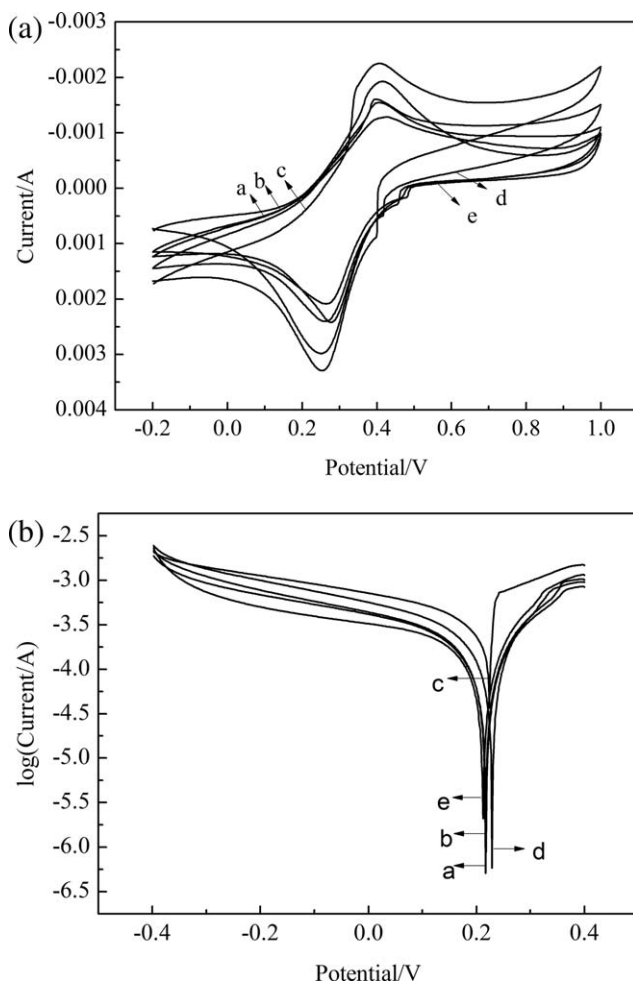


**Figure 3.** CV curves and Tafel polarization curves of P(2,3-DMA) at different mole ratio of APS to 2,3-DMA;  $n(\text{APS})/n(2,3\text{-DMA})$ : a: 1 : 1; b: 1.5 : 1; c: 2 : 1; d: 2.5 : 1; e: 3 : 1.

Figure 1 illustrates the plot of cyclic voltammetry and Tafel polarization of P(2,3-DMA), which doped with different  $\text{H}_3\text{PO}_4/2,3\text{-DMA}$  mole ratio. It is observed from the cyclic voltammogram that there is a pair of redox peaks, the potential of oxidation peak was about 0.41 V, the potential of reduction peak at about 0.23 V, the difference ( $\Delta E = E_{\text{pa}} - E_{\text{pc}}$ ) is 0.18 V, it indicates that the electrochemical behavior of P(2,3-DMA) is quasi reversible not reversible completely. After 100 times of scanning, the potential and current of the redox peak has no change; moreover, the carbon paper loaded P(2,3-DMA), which was placed in the air for 30 days has the same redox peak with the Figure 1, so it indicates that the P(2,3-DMA) has excellent electrical activity and chemical stability.

It is found from Figures 1 and 2 that the peak current of cyclic voltammogram, the corrosion potential of Tafel polarization, and the polymerization yield have the same trend. They increase with the increase of  $n(\text{H}_3\text{PO}_4)$ , reach maximum, and then decrease. And, the optimum ratio of  $n(\text{H}_3\text{PO}_4)/n(2,3\text{-DMA})$  is 2.5. This maybe due to the polymerization reaction easily in the acidic conditions. The higher concentration of  $\text{H}_3\text{PO}_4$  progress-

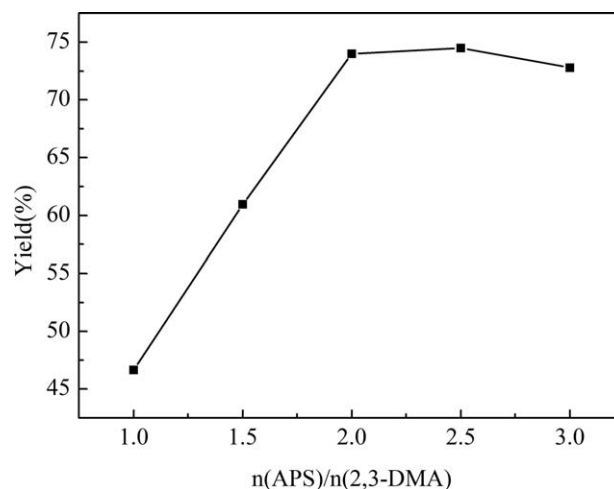


**Figure 4.** The relation between the yield of P(2,3-DMA) and the mol ratio of APS to 2,3-DMA;  $n(\text{APS})/n(2,3\text{-DMA})$ : a: 1 : 1; b: 1.5 : 1; c: 2 : 1; d: 2.5 : 1; e: 3 : 1.

ing the polymerization speed, the molecular weight of P(2,3-DMA) will be higher with the increase of reaction speed, so the electrochemistry properties will be better, furthermore, the

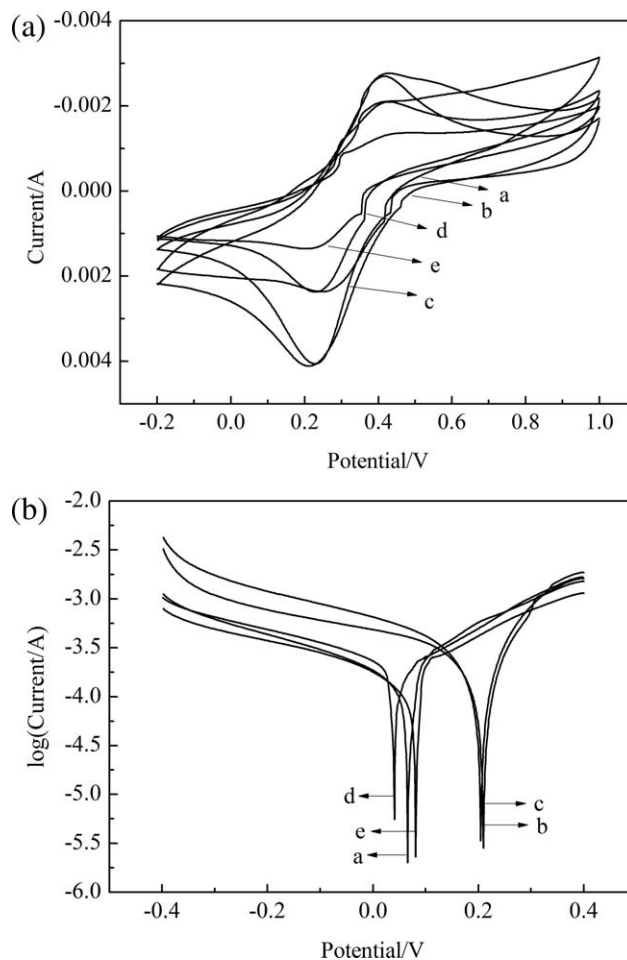


**Figure 5.** CV curves and Tafel polarization curves of P(2,3-DMA) at different temperature: a: 10°C; b: 20°C; c: 30°C; d: 40°C; e: 50°C.

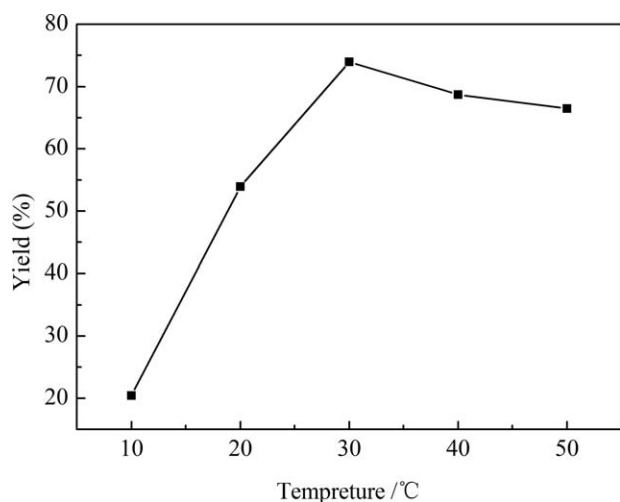


**Figure 6.** The relation between the yield of P(2,3-DMA) and temperature: a: 10°C; b: 20°C; c: 30°C; d: 40°C; e: 50°C.

doped degree will increase with the increase of the concentration of  $H_3PO_4$ , and the polymerization yield will be higher. The excess acid inhibits the reaction process. The yield and the elec-

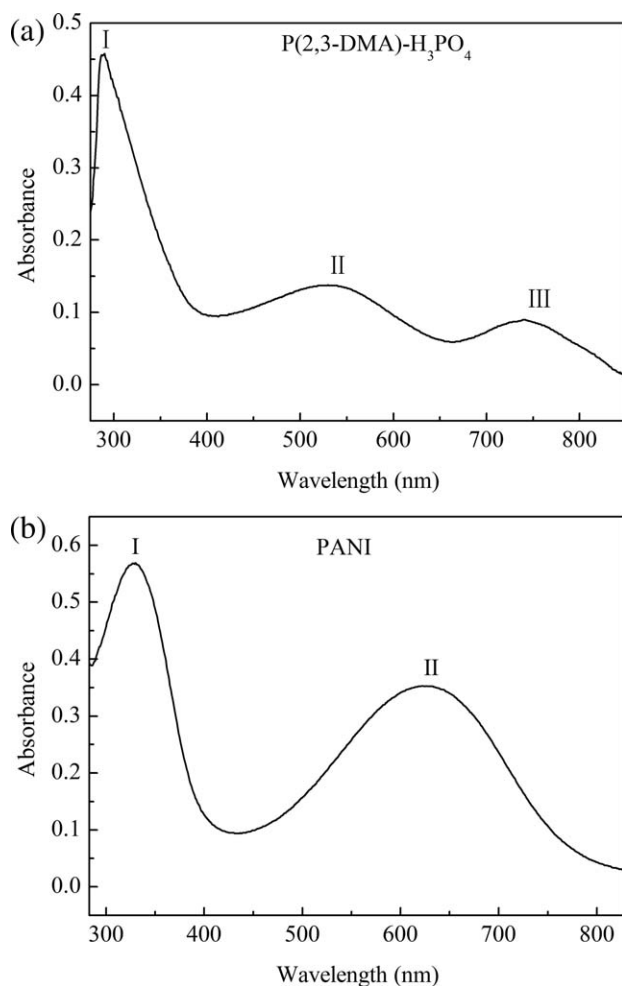


**Figure 7.** UV-vis spectra of P(2,3-DMA) and PANI.

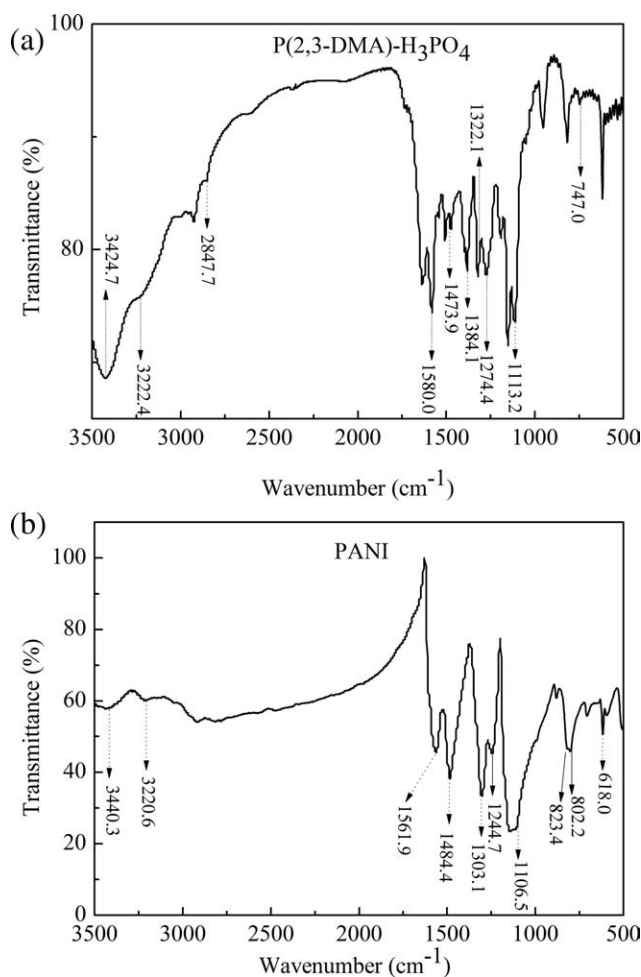


**Figure 8.** FTIR spectra of P(2,3-DMA) and PANI.

trochemistry properties decrease significantly. In addition, the electrochemistry property and the polymerization yield of P(2,3-DMA) have a relationship with the doped degree.

**Effect of APS/2,3-DMA Ratio.** The effect of the oxidant/monomer mole ratio on the electrochemical property and the polymerization yield of P(2,3-DMA) was studied by changing the ratio from 1/1 to 3/1 (Figures 3 and 4).

As shown in Figures 3 and 4, the cyclic voltammogram peak current and Tafel polarization of P(2,3-DMA) and the polymerization yield have the same trend. They all increase with the increase of APS. The optimum ratio of  $n(\text{APS})$  to  $n(2,3\text{-DMA})$  was 2. A further increase of APS beyond optimum leads to a slight decrease in electrochemical properties and yield. The APS is the initiator and oxidizing agent. So, more oxidant is beneficial to the formation of the 2,3-DMA cation radical with higher polymerizability, promoting chain propagation reaction, and then increasing the length of polymer chain and polymerization yield. So, at the optimum ratio, the current of redox peak is highest, and the potential of Tafel polarization shifts to anionic side and the yield is the highest. Less oxidant will result in formation of the less polymerizing active centers, favoring the

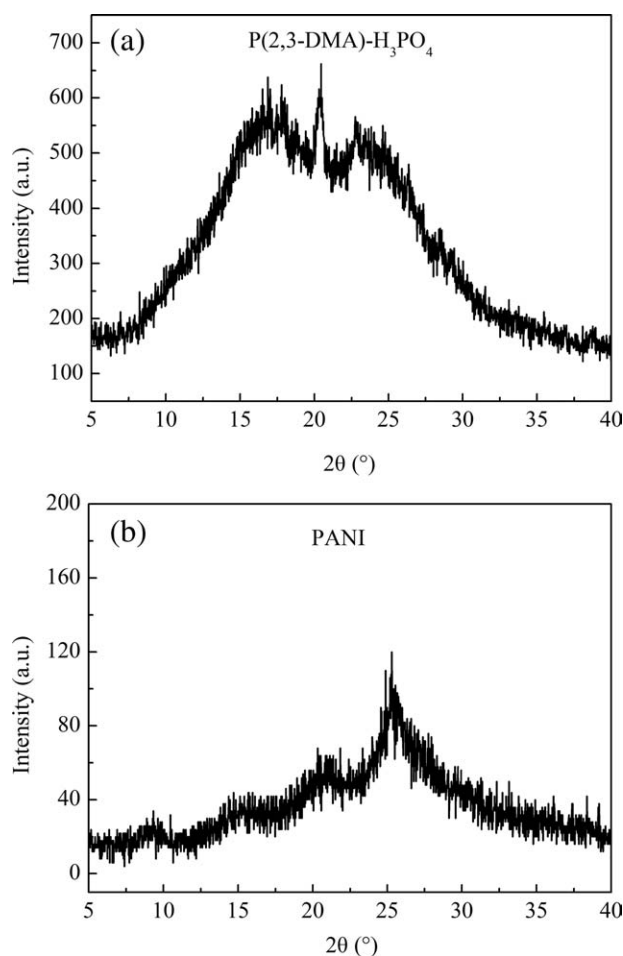


**Figure 9.** XRD patterns of P(2,3-DMA) and PANI.

chain propagation reaction but lowering polymerization yield. The excess oxidant bring too much active centers, the polymerization speed will be too fast and the low weight molecular chain will be more due to self-annihilation of the growing polymeric chains, thus the electrochemistry properties and the yield of P(2,3-DMA) will declined.

**Effect of Temperature.** To examine the effect of temperature on the electrochemical property and polymerization yield of P(2,3-DMA), the polymerization was performed at 10°C, 20°C, 30°C, 40°C, and 50°C (Figures 5 and 6).

As shown in Figures 5 and 6, the polymerization temperature has a strong effect on the electrochemistry properties and polymerization yield of the P(2,3-DMA). It is observed that the current of cyclic voltammogram redox peak increase with the

**Table I.** The Solubility of PANI and P(2,3-DMA) in Different Solvents (25°C)

| Polymers solubility (mg/mL) | Solvent  |         |
|-----------------------------|----------|---------|
|                             | Acetidin | Ethanol |
| PANI                        | 0.89     | 1.47    |
| P(2,3-DMA)                  | 3.47     | 6.08    |

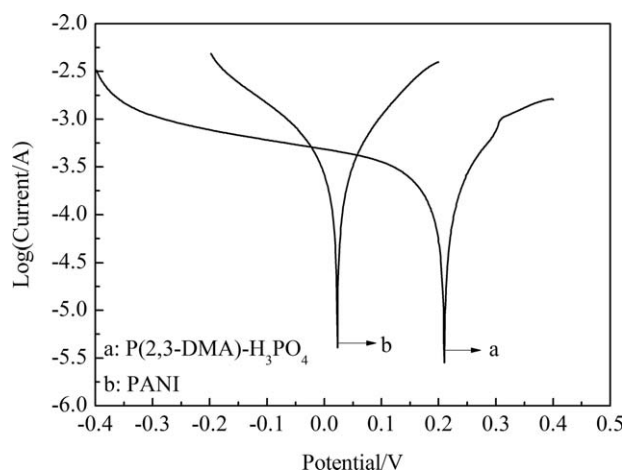


**Figure 10.** Tafel polarization curves of PANI and P(2,3-DMA).

increasing temperature, give the maximum current at 30°C, a further rise in temperature leads to a decrease in the current of redox peak. The Tafel polarization curves and the polymerization yield curve have the same trend with the cyclic voltammogram curves, because the higher temperature will fast the reaction speed, promote chain propagation reaction, and then increase the length of polymer chain and polymerization yield. Lower temperature results the delayed formation of active centers, leading to the depression electrochemistry properties and the yield of the P(2,3-DMA). The polymerization reaction completes fast when the temperature is beyond 30°C. And, side reaction may occur at the elevated temperature, leading to the depression of the polymerization yield.

### Structure Analysis and Properties of the P(2,3-DMA)

**UV-Vis Spectroscopy Analysis.** The UV-vis absorption spectra of P(2,3-DMA) and PANI is shown in Figure 7. The UV-vis absorption spectra of P(2,3-DMA) doped with H<sub>3</sub>PO<sub>4</sub> shows three characteristic absorption bands, at 740–760 (III), 530–550 (II), and 290–305 (I) nm wavelengths, respectively. The absorption Bands III and II are mainly assigned to polaron transition. The absorption Band I arises from  $\pi$ - $\pi^*$  electron transition within the benzoid segments. The UV-vis spectra of PANI exhibits two bands at 620–630 (II) and 325–335 (I) nm, respectively. This is agreement with Refs. 15–17. The absorption Band II is assigned to  $n$ - $\pi^*$  transition in the molecular structure. The absorption Band I is due to  $\pi$ - $\pi^*$  electron transition within the benzoid segments.

It can be seen from Figure 7 that the P(2,3-DMA) has the similar structure with the PANI. But, the absorbance peaks of P(2,3-DMA) shows a blue shift to some extent. The possible reason is that the 2,3-ortho-substituted benzene ring, hence increasing the steric volume. So, the  $\pi$ - $\pi^*$  transition needs more energy, the molecular conjugate degree were lower.

**Infrared Spectroscopy Analysis.** Figure 8 shows the infrared spectrum of P(2,3-DMA) and PANI.

From the spectrum of P(2,3-DMA) in Figure 8, it is observed that the characteristic peaks of P(2,3-DMA) occur at 3424.7, 3222.4, 2847.7, 1580.0, 1473.9, 1384.1, 1322.1, 1274.4, 1113.2,

**Table II.** The Corrosion Potential ( $E_{\text{corr}}$ ) and Corrosion Current ( $I_{\text{corr}}$ ) of PANI and P(2,3-DMA)

| Samples    | $E_{\text{corr}}$ (V) | $I_{\text{corr}}$ (A)  |
|------------|-----------------------|------------------------|
| P(2,3-DMA) | 0.209                 | $2.132 \times 10^{-4}$ |
| PANI       | 0.022                 | $4.187 \times 10^{-4}$ |

and  $747.0 \text{ cm}^{-1}$ . The peak at  $3424.7 \text{ cm}^{-1}$  is assigned to the N—H stretching vibration. The peak at  $3222.4 \text{ cm}^{-1}$  is assigned to the C—H stretching vibration of aromatic rings. The peak at  $2847.7 \text{ cm}^{-1}$  is due to the saturated alkyl C—H stretching vibration, and the peak at  $1380 \text{ cm}^{-1}$  is assigned to the  $-\text{CH}_3$  characteristic absorption, these data shows that there are methyl substituents in the polymer backbone. The peaks at  $1580.0$  and  $1473.4 \text{ cm}^{-1}$  are characteristic of quinoid and benzenoid rings. And, the peaks at  $1322.1$  and  $1274.4 \text{ cm}^{-1}$  are characteristic of C—N stretching vibrations of quinoid and benzenoid rings in the polymer backbone. The two peaks at  $1113.2$  and  $747.0 \text{ cm}^{-1}$  are due to in plane and out of plane C—H bending vibration.

The spectrum of PANI in Figure 8 shows characteristic peaks at  $3440.3$ ,  $3220.6$ ,  $1561.9$ ,  $1484.4$ ,  $1303.2$ ,  $1244.7$ ,  $1106.5$ , and  $802.2 \text{ cm}^{-1}$ . Compared with the IR spectra of PANI, it is observed that the structure of the P(2,3-DMA) is similar to PANI,<sup>18–20</sup> both of them have the benzene and quinone ring structure crossing connected with N atoms, the difference were there are methyl characteristic peaks in IR spectra of P(2,3-DMA) and the peaks of P(2,3-DMA) shows a bathochromic shift. This is because the molecular steric volume of P(2,3-DMA) is much bigger, hence suggesting shorter molecular conjugated chain. So, the methyls have influence on the conjugated degree of the molecular chains, the distribution of the electron cloud is nonuniform.

**XRD Analysis.** Figure 9 is the XRD of P(2,3-DMA) and PANI. It can be found that the P(2,3-DMA) exhibits three sharper diffraction peaks at  $2\theta = 17^\circ$ ,  $20^\circ$ , and  $23^\circ$ , and the PANI shows four diffraction peaks at  $2\theta = 9.2^\circ$ ,  $15.5^\circ$ ,  $20.7^\circ$ , and  $25.3^\circ$ . The diffraction peaks of PANI is consistent with the researches.<sup>20</sup> From the data, we can see that the P(2,3-DMA) and the PANI were both partially crystalline, the structure of them were similar.

**The Solubility Studies.** It can be seen from Table I that the P(2,3-DMA) exhibits a much better solubility than the PANI in the low-boiling point solvents, hence suggesting that the methyl-substituted benzene ring also plays an important role in the solubility, mainly due to the rigidity of P(2,3-DMA) molecular chain decreased because of the larger steric volume, and the P(2,3-DMA) has lower molecular weights than PANI.

**The Tafel Polarization Studies.** Figure 10 is the Tafel plots of carbon paper loaded PANI and P(2,3-DMA), The corrosion potential ( $E_{\text{corr}}$ ) and corrosion current ( $I_{\text{corr}}$ ) were showed in Table II.

The Tafel plots is the typical measurement to investigate the anticorrosion properties of the polymers.<sup>21</sup> It can be found that the  $E_{\text{corr}}$  of P(2,3-DMA) has a considerable shift toward anodic side, the  $I_{\text{corr}}$  are significantly lower than PANI. The results

show that the anticorrosion properties of P(2,3-DMA) better than PANI. This phenomenon gives us a hint that the P(2,3-DMA) can be used as an anticorrosion additive.

## CONCLUSION

P(2,3-DMA) have been chemically synthesized using  $\text{H}_3\text{PO}_4$  as the doped acid. The polymerization yield, Tafel polarization, and cyclic voltmmatry depend significantly on the  $\text{H}_3\text{PO}_4$  concentration, oxidant/monomer ratio, and polymerization temperature. The optimized  $\text{H}_3\text{PO}_4$ /monomer ratio, oxidant/monomer ratio, and temperature for the preparation with a high yield, better electrochemical properties are 2.5/1, 2/1, and  $30^\circ\text{C}$ , respectively. The UV-vis, IR spectra, and XRD exhibit the structure of P(2,3-DMA) is similar with PANI. Moreover, the solubility analysis indicates that P(2,3-DAM) has better solubility than PANI because of the 2,3-ortho-substitute-benzene ring lead to the larger steric volume among molecular chains. And fortunately, the anticorrosion properties of P(2,3-DMA) were better than PANI.

## REFERENCES

- Pud, A.; Ogurtsov, N.; Korzhenko, A.; Shapoval, G. *Prog. Polym. Sci.* **2003**, *28*, 1701.
- Sambhu, B.; Dipak, K.; Nikhil, K. S.; Joong, H. L. *Prog. Polym. Sci.* **2009**, *34*, 783.
- Sathiyarayanan, S.; Muthukrishnan, S.; Venkatachari, G.; Trivedi, D. C. *Prog. Org. Coat.* **2005**, *53*, 297.
- Li, X. G.; Huang, M. R.; Duan, W.; Yang, Y. L. *Chem. Rev.* **2002**, *102*, 2925.
- Savithaa, P.; Sathyanarayana, D. N. *Synth. Met.* **2003**, *145*, 113.
- Savitha, P.; Sathyanarayana, D. N. *Polym. Int.* **2004**, *53*, 106.
- Santhosh, P.; Sankarasubramanian, M.; Thanneermalai, M.; Gopalan, A.; Vasudevan, T. *Mater. Chem. Phys.* **2004**, *85*, 316.
- Umare, S. S.; Borkar, A. D.; Gupta, M. C. *Bull. Mater. Sci.* **2002**, *25*, 235.
- Bergeron, J. Y.; Dao, L. H. *Macromolecules* **1992**, *25*, 3332.
- Tom, L.; Ari, I. J. *Electroanal. Chem.* **2002**, *531*, 43.
- Anjali, A. A.; Milind, V. K. *Sens. Actuators B* **2000**, *67*, 173.
- Vandana, S.; Sainkar, S. R.; Gangal, S. A.; Patil, P. P. *J. Mater. Sci.* **2006**, *41*, 2851.
- Ma, L.; Luo, L. Z.; Gan, M. Y.; Li, X. F.; Su, W. Y.; Yan, J.; Tang, J. H. *Acta Chim. Sinica* **2010**, *68*, 814.
- Yoon, C. O.; Kim, J. H.; Sung, H. K.; Lee, H. *Synth. Met.* **1997**, *84*, 789.
- Shreepathi, S.; Holze, R. *Chem. Mater.* **2005**, *17*, 4078.
- Kim, Y. B.; Choi, J. K.; Yu, J. W. *Synth. Met.* **2002**, *79*, 131.
- Subrahmanya, S.; Rudolf, H. *Langmuir* **2006**, *22*, 5195.
- Šeděnková, I.; Trchová, M.; Blinova, N. V.; Stejskal, J. *Thin Solid Films* **2006**, *515*, 1640.
- Zhang, J.; Shan, D.; Mu, S. L. *Polymer* **2007**, *48*, 1269.
- Li, G. C.; Zhang, Z. K. *Macromolecules* **2004**, *37*, 2683.
- Kunal, S.; Jude, I. *Synth. Met.* **2002**, *132*, 35.